

This suggests that a physically more meaningful expression for B^2 can be obtained by a rearrangement of Eq. (3) giving

$$B^2 = \frac{[k_t/(1 - k_r)] - 1}{L^2 + [1/(1 - k_r)]\tau} \quad (3b)$$

with increased fast leakage arising from the increased fast-to-thermal flux ratio.

If the two-group equations are written in the time-dependent form, omitting the complications arising from the delayed neutrons, then the reactor time constant, λ , can be shown to have the form

$$\lambda = \frac{1}{l_t} \left[\frac{k_t}{1 - k_r + \tau B^2} - (1 + L^2 B^2) \right] \quad (5)$$

where l_t is the thermal neutron lifetime, and $l_t \gg l_f$.

It is of note that from Eq. (4) the ratio of resonance to thermal captures in the fertile material is increased by a factor of $1/(1 - k_r)$ as compared to the usual formulation.

In the above, it has been assumed throughout that the resonance captures in fertile material come at higher energies than those in the fissile material. If this is not a good model of the actual process, then p_{28} in the expression for k_r may properly be somewhat larger than in the expression for k_t .

P. F. GAST

*Hanford Atomic Products Operation
General Electric Company
Richland, Washington*

Received September 12, 1960

Prediction of Thermal-Neutron Fluxes in the Bulk Shielding Facility from Lid Tank Shielding Facility Data

In order to obtain the maximum usefulness from shielding data collected at either the Lid Tank Shielding Facility (LTSF) or the Bulk Shielding Facility (BSF), the power of the experimental source must be accurately known. Furthermore, the data must be correctly converted by geometrical transformations from the experimental source to the reactor for which the shield is being designed. One method for checking the powers quoted for the LTSF source (a disk-shaped uranium plate) and the BSF reactor, as well as a method for checking on the validity of the geometrical transformations, is to perform a calculation predicting the neutron flux in the BSF on the basis of LTSF data transformed first to a point-to-point kernel and then to the geometry of the BSF reactor. A discrepancy between the predicted and the measured fluxes would indicate either that one of the quoted powers was in error or that the geometrical transformations were not properly derived.

A calculation (1) that compared the fast-neutron doses was performed in 1952. Since neither the power of the Bulk Shielding Reactor (BSR) nor the power of the LTSF source

plate was accurately known at that time, it was not surprising that the calculated and experimental results were not in agreement. Re-estimates of both the power of the BSR (2) and the power of the LTSF source plate (3) have since become available, however, and a second calculation has been made in which the thermal-neutron fluxes at the two facilities have been compared.

Before a conversion from LTSF data to BSF data could be made it was necessary to obtain information about the self-attenuation of neutrons inside the BSR. This was done by placing an all-aluminum mockup of one layer of fuel elements of the BSR adjacent to the source plate in the LTSF and taking thermal-neutron measurements in the water beyond the mockup. Three configurations were used: no mockup; a nine-plate mockup (one-half of a layer of elements); and an 18-plate mockup (a full layer of elements).

Since the experimental data were for a plane disk source it was necessary to convert it to a point source geometry by the standard transformation (4):

$$G(z) = \sum_{\nu=0}^{\infty} B(\sqrt{z^2 + \nu a^2}) \quad (1)$$

where

$$B(z') = -\frac{1}{2\pi S z'} \frac{d}{dz'} D_{pl}(z', a)$$

$$z' = \sqrt{z^2 + \nu a^2}$$

$G(z)$ = attenuation kernel for a point fission source at a distance z from the detector, neutrons/cm²/sec/watt

S = LTSF specific source strength, watts/cm²

$D_{pl}(z, a)$ = flux at a distance z from the disk, neutrons/cm²/sec

a = radius of disk = 35.56 cm

The source strength of the Lid Tank disk was taken to be 5.22 w $\pm 5\%$, the value quoted by Otis (3). Since Otis calculated the source plate leakage factor for neutrons to be 0.94, the actual source strength value used was 4.91 w. The assumption was also made that the source plate power was uniform over the whole disk. Otis calculated that the source power was constant within approximately 10% from the mean.

Thermal-neutron flux attenuation kernels were calculated for the three configurations measured from Eq. (1) and then extrapolated for fuel element thicknesses up to six elements, which was the thickness of the BSR Loading 33. This extrapolation was made approximately linear on semilog graph paper. The error involved here was kept low by the fact that the largest portion of the measured flux in the BSF came from elements near the front face of the reactor core.

Equation (1) was not accurate for distances greater than about 100 cm from the source plate, however, since, in order to compute $G(z)$, it was necessary to have a knowledge of the flux, D , for fairly large distances beyond z , and such measurements were not made at points farther out than 150 cm from the source plate.

The flux data was therefore extrapolated out to about 190 cm before this calculation was performed. In order to check the validity of this extrapolation, the kernels were

also computed using the following approximate formula (5):

$$G(z) = \left(\frac{1}{4\pi z S \lambda} + \frac{1}{\pi a^2 S} \right) D_{pl}(z, a) \quad (2)$$

where λ , the neutron relaxation length in the LTSF, is defined as

$$\lambda(z) = - \frac{D_{pl}(z, a)}{(d/dz) [D_{pl}(z, a)]}$$

Equation (2) assumes that λ is only slowly varying in z .

At 100 cm the approximate and exact kernels differ by about 5%, but the two kernels become closer in value for larger distances.

A check of the geometrical transformation given by Eq. (1) was made by integrating the point kernels thus obtained over the Lid Tank source plate and then comparing them with the original flux data. The results of this integration furnish good evidence of the validity of the geometrical transformation used. The agreement was $\pm 5\%$ for distances less than 135 cm, well within the accuracy of the measurements of the flux.

The flux to be expected at a distance z from a reactor of any shape can be represented approximately by

$$D(R) = \iiint_{\text{reactor volume}} p(R_1) G(R, R_1) dR_1 \quad (3)$$

where

- R = vector position of detector
- R_1 = vector position in reactor
- $p(R_1)$ = power density at R_1
- $G(R, R_1)$ = dose at R due to unit source at R_1 , taking account of the difference in materials in the core and shield.

Since the power distribution through the BSF reactor was irregular, it could not be described by a single mathematical expression. Therefore the reactor was divided into 304 volume elements and the power in each volume element was computed. These calculations were based on mappings of the thermal-neutron fluxes in the reactor that were reported by Johnson (2). The sum of powers in these volume elements was 26.8 kw, which was in reasonable agreement with the 27.3 kw reported by Johnson.

The flux at a distance R from the center of the north face of the BSR was approximated by

$$D(R) = \sum_{\mu=1}^{40} \sum_{\nu=1}^8 p_{\mu\nu} G(R_{\mu\nu}) \quad (4)$$

where

- μ = number of each volume in a particular layer
- ν = number of the layer
- $p_{\mu\nu}$ = average power density of the volume element $\mu\nu$
- $R_{\mu\nu}$ = distance to the center of the volume element $\mu\nu$

The $G(R_{\mu\nu})$ were obtained from the fuel element mockup data by referring to the curve that corresponded to the given thickness of fuel element attenuation. The assumption

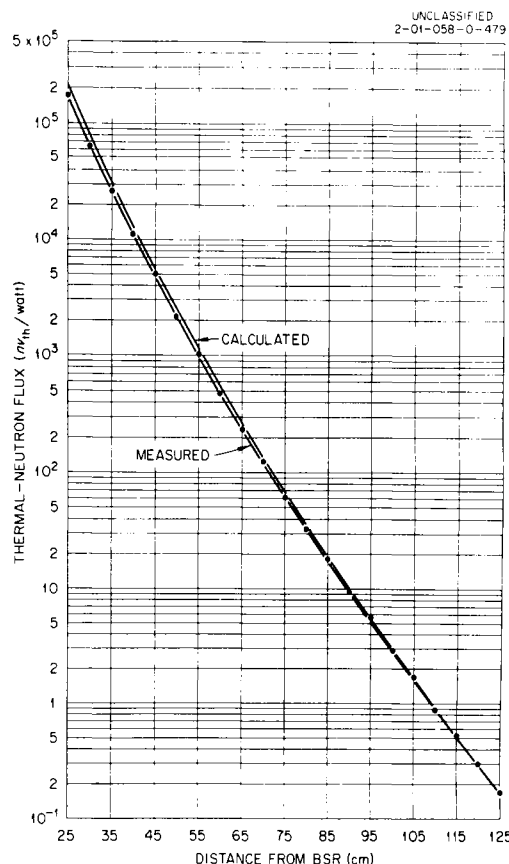


FIG. 1. Comparison of predicted and measured thermal-neutron fluxes near the bulk shielding reactor.

was made that the self-attenuation of each element was small and that $G(R_{\mu\nu})$ was therefore a reasonable approximation of the mean attenuation kernel for the entire volume element. The size of element used was chosen as a compromise between the desire for accuracy in this phase and the fact that the BSR flux data had to be interpolated over these elements.

The results of the calculation are compared with experimental measurements in Fig. 1. At a distance of 25 cm from the reactor the predicted flux is too high by a factor of 1.18, while for a distance of 125 cm the predicted flux is too low by 6%. The agreement between the measured and calculated fluxes appears to be good for the larger distances, but there is a discrepancy of 12 to 22% for distances closer than 60 cm from the reactor. There is a possibility that the size of volume element used in the approximate integration over the reactor was too large to be accurate for these distances, or that extrapolation errors of the attenuation kernels were greater for closer distances. Also, the possibility of the source calibrations being in error is not completely discounted. This will be partially answered by a recalibration of the BSR now being planned. Since the self-attenuation data were based on pure aluminum dummy elements, the absence of U^{235} in the elements might affect the results close to the reactor. The comparison should be valid for large distances, since the thermal-neutron flux at water at distances greater than about 25 cm from the source depends only on the fast-neutron flux.

The details of this calculation are presented elsewhere (6).

REFERENCES

1. T. A. WELTON AND E. P. BLIZARD, *Reactor Sci. Technol.* **2**(2), 73 (1952) (classified).
2. E. B. JOHNSON, Power calibration for BSR loading 33. ORNL-CF-57-11-30 (1957).
3. D. R. OTIS, Lid tank shielding facility at the Oak Ridge National Laboratory, Part II, determination of the fission rate of the source plate. ORNL-2350 (1959).
4. E. P. BLIZARD, Transformation from disc to point source geometry. ORNL-CF-52-3-219 (1952).
5. E. P. BLIZARD, "Nuclear Radiation Shielding" (Harold Etherington, ed.), pp. 7-94. McGraw-Hill, New York, 1958.
6. A. D. MAC KELLAR, Prediction of thermal-neutron fluxes near the bulk shielding reactor from lid tank shielding facility data. ORNL-CF-59-1-24 (1959).

A. D. MAC KELLAR

Oak Ridge National Laboratory*
Oak Ridge, Tennessee
Received November 25, 1960

* Operated by Union Carbide Corporation for the U. S. Atomic Energy Commission.

Failure of Neutron Transport Approximations in Small Cells in Cylindrical Geometry

A common problem in reactor design is the calculation of the thermal-neutron flux fine structure in fuel element cells. When the cell dimensions become less than a mean free path, it has been popular to use P_n and S_n approximations to the Boltzman equation, rather than diffusion theory, P_1 . However, it has been found that in cylindrical geometry, approximations such as P_3 , S_4 , and S_8 , can in some instances be poorer than P_1 . This is not in contradiction to many successful comparisons of P_3 with experiment. The latter have typically been loosely packed, room-temperature lattices; the cases studied here are tightly packed lattices with a low-density coolant, as might be encountered in some power reactors.

TABLE I
LATTICE CHARACTERISTICS

Lattice No.	Spacing, a , (in cm)	Void fraction, γ	H ₂ O cross sections, cm ⁻¹	
			Σ_{a^1}	Σ_{tr^1}
1	1.524	0.25	0.0088	1.053
2		0.5	0.00587	0.702
3		0.25	0.0088	1.053
4	1.143	0.5	0.00587	0.702
5		0.75	0.00293	0.351
6		0.95	0.000587	0.0702

Table I gives characteristics of lattices arbitrarily chosen for study. These are all 1.5% enriched uranium metal rods, 0.3 in. in diameter, and separated by a distance, a , in a square lattice. In all cases $\Sigma_{a^0} = 0.387$ cm⁻¹ and $\Sigma_{tr^0} = 0.393$ cm⁻¹ for the fuel. Boiling light water with a 600 psig density, 0.8 (1 - α), is assumed to be the coolant. α is the void fraction. Lattices near the bottom of the table are unlikely in practical reactors, but are useful in this study. The choice of a Maxwellian spectrum at 0.045 ev, for all lattices, simplifies the study and does not affect the conclusions.

Methods used to compute the fine structure in these cells having a constant source in the coolant are as follows:

1. Monte Carlo (1). This is two dimensional, (xy), and it is necessary to approximate the fuel rod as a square with the corners removed.
2. Amouyal's approximation (2). This uses cylindrical geometry diffusion theory in the coolant and transport theory in the fuel.
3. Diffusion theory in cylindrical geometry (which gives the same result as diffusion theory in the equivalent one-dimensional slab geometry).
4. P_3 in cylindrical geometry.
5. S_3 in cylindrical geometry.
6. S_4 in cylindrical geometry.
7. S_8 using an equivalent one dimensional slab geometry.
8. P_3 using an equivalent one dimensional slab geometry.

Regarding the S_n methods, these exist in two forms, the so-called SNG and the DSN (3) and both are examined here.

In methods having an outer cell boundary which is cylindrical, the cell radius, r_1 , as obtained from

$$\pi r_1^2 = a^2 \quad (1)$$

To obtain the half-thicknesses of the equivalent fuel and coolant slabs, δ_0 and δ_1 , from the fuel and cell radii, r_0 and r_1 , the criteria

$$\bar{\phi}_{fuel} : \phi_{fuel \text{ edge}} = C_1; \phi_{fuel \text{ edge}} : \bar{\phi}_{coolant} = C_2 \quad (2)$$

can be applied to cylindrical and slab geometries using diffusion theory, requiring that C_1 and C_2 be the same in both geometries, with the approximate results:

$$\delta_0 \cong \sqrt{\frac{3}{8}} r_0 \quad (3)$$

$$\delta_1 \cong \frac{\sqrt{6} r_0}{1 - \left(\frac{r_0}{r_1}\right)^2} \left\{ \frac{\ln \frac{r_0}{r_1}}{1 - \left(\frac{r_0}{r_1}\right)^2} - \frac{3}{4} + \frac{1}{4} \left(\frac{r_0}{r_1}\right)^2 \right\} \quad (4)$$

Tables II and III give the results of these methods for selected lattices from Table I. The P_1 results in Table III are the same as those of Table II by virtue of the definition of slab equivalence. The meaning of the error assigned to the monte carlo results is that the band defined has a 95% chance of encompassing the true answer. If monte carlo is regarded as correct the following inferences can be made.

(a) While possibly for larger lattice sizes (in terms of